Published in final edited form as:
Electroanalysis. 2012 October ; 24(10): . doi:10.1002/elan.201200302.

Manganese Detection with a Metal Catalyst Free Carbon Nanotube Electrode: Anodic versus Cathodic Stripping Voltammetry

Wei Yue[a], **Adam Bange**[b], **Bill L. Riehl**[c], **Bonnie D. Riehl**[c], **Jay M. Johnson**[c], **Ian Papautsky**[d], and **William R. Heineman**[*,a]

[a]Department of Chemistry, University of Cincinnati, Cincinnati, OH, 45221-0172, USA

[b]Department of Chemistry, Xavier University, Cincinnati, OH, 45207, USA

[c]SCNTE LTD P.O. Box 38, Alpha, OH 45301, USA

[d]BiomicroSystems Labs, School of Electronic and Computing Systems, University of Cincinnati, Cincinnati, OH, 45221-0030, USA

Abstract

Anodic stripping voltammetry (ASV) and cathodic stripping voltammetry (CSV) were used to determine Mn concentration using metal catalyst free carbon nanotube (MCFCNT) electrodes and square wave stripping voltammetry (SWSV). The MCFCNTs are synthesized using a Carbo Thermal Carbide Conversion method which results in a material that does not contain residual transition metals. Detection limits of 120 nM and 93 nM were achieved for ASV and CSV, respectively, with a deposition time of 60 s. CSV was found to be better than ASV in Mn detection in many aspects, such as limit of detection and sensitivity. The CSV method was used in pond water matrix addition measurements.

Keywords

Manganese; Anodic stripping voltammetry; Cathodic stripping voltammetry; Metal catalyst free carbon nanotube electrode

1 Introduction

Manganese (Mn) is commonly found throughout most aquatic environments. While Mn is a required trace metal, elevated concentrations of Mn are associated with a host of health issues, including neurotoxicity and development of Parkinson's disease symptoms [1,2]. For this reason, Mn in drinking water is regulated at a low concentration of 50 ppb, and thus the determination of Mn in aqueous samples is of direct practical importance [3].

Both spectroscopic and electroanalytical methods are commonly used for the determination of trace metal contaminants such as Mn; both methods offer advantages for different applications. Typically, electroanalytical methods are less expensive, more portable, and require fewer separation steps than spectroscopic techniques. The electroanalytical technique most commonly used for the determination of metal analytes at the trace level is stripping voltammetry.

[*]heinemwr@uc.edu.

Stripping voltammetry broadly describes a variety of electroanalytical techniques that are often used for many analytical applications where a high level of sensitivity is required. Stripping methods are generally more sensitive than other voltammetric techniques because of a preconcentration step which accumulates the desired analyte on the surface of the electrode. The analyte may be preconcentrated by either electrodeposition or by physical adsorption, depending on the analyte and the stripping method being used. Once sufficient preconcentration is achieved, the potential of the working electrode is swept as to strip the analyte off of the electrode surface, with the associated faradaic current being measured to quantitatively determine the concentration of analyte present [4].

ASV is the most commonly used form of stripping voltammetry. In this technique the analyte, typically a metal ion, is preconcentrated on the electrode surface by reductive electrodeposition. The electrode potential is then swept in the positive direction, and metal ions are oxidatively liberated from the electrode surface at their oxidation potentials [5,6]. The determination of numerous metals has been reported using ASV, on solid electrode surfaces as well as on liquid films and drops of mercury [5,7]. While most commonly applied to metals such as copper, cadmium, lead, and zinc, ASV has also been used for the determination of Mn [8]. Mn is more difficult to determine by ASV in some applications because of the negative potential of the $Mn^{2+} + 2e^{-} \rightarrow Mn$ redox couple. This reduction potential is beyond the working range of most common solid electrode materials, and most reported ASV methods use a Hg surface [4,6,8]. Due to toxicity concerns, the use of Hg is often limited, making these analyses unsuitable for many applications [9–12].

A second form of stripping voltammetry that has been used for Mn determination is adsorptive stripping voltammetry (AdSV) [13,14]. In AdSV, the deposition of the analyte is not accomplished by means of electrolysis, but rather by a physical or chemical interaction with the electrode surface. Many of the AdSV techniques for Mn that have been reported in the literature use Hg, making these techniques unsuitable for applications requiring mercury-free analysis [14].

CSV is a third stripping technique used for Mn determination [15–17]. CSV is the reverse of ASV in that the analyte is accumulated as an oxidized species, and is stripped by a potential sweep in the negative direction. This technique offers several advantages for Mn determination, including insensitivity to oxygen and intermetallic interferences, Hg free analysis, and a redox potential within the working range of many common electrode materials. CSV methods have been reported using glassy carbon, platinum, and boron doped diamond electrodes [15,18,19].

Recently, carbon nanotubes (CNTs) have emerged as a novel electrode material due to their useful electrochemical properties, such as large potential window, fast electron transfer rate and large surface area [20–22]. CNT electrodes have been created in a number of ways, including arc discharge, laser ablation and chemical vapor deposition [23,24]. A hindrance of these methods when producing electrodes for trace stripping analysis is that they generally use metal catalysts that can contaminate the CNTs and reduce the analytical effectiveness for sensor applications [25–27]. Previously, metal catalyst free CNTs (MCFCNTs) synthesized via a solid-phase growth mechanism has been reported by the Banks research group [28]. CNTs are grown on a silicon carbide matrix which does not have a residue of transition metal catalyst in the CNT structure [28,29]. Because of its unique array structure, this novel material is very robust and the CNTs can be “rejuvenated” by refreshing the electrode with a high voltage treatment [30]. In this paper, the use of MCFCNT electrodes for trace determination of Mn using ASV and CSV is explored.

2 Experimental

All chemicals were purchased without further purification: Mn AAS standard solution with 2% HNO_3 from Fisher Scientific, 20X borate buffer from Thermo Scientific. MCFCNT electrodes were supplied by SCNTE LLC (Beavercreek, OH) and used without any pretreatment. All solutions were prepared with deionized water (18.2 MΩ from Milli-Q System, Barnstead, MA). ASV measurements were carried out in a 20 ml conventional three-electrode cell consisting of MCFCNT electrode as working electrode, Ag/AgCl as reference electrode (filled with 3 M KCl solution), Pt wire as auxiliary electrode. The solution volume was 15 ml for both ASV and CSV experiments. A BASi 100B Electrochemical Analyzer from BASi (West Lafayette, IN) was used as the potentiostat. Basic set-up parameters for Osteryoung square wave voltammetry were S. W. amplitude=25 mV, step potential=5 mV and frequency=25 Hz [31].

3 Results and Discussion

3.1 Anodic Stripping Voltammetry Study of Manganese

3.1.1 Cyclic Voltammetry of Mn in NH_4Cl—ASV of Mn in NH_4Cl has been done and shown to give repeatable and reliable results on a rotating solid silver amalgam electrode in 0.05 M NH_4Cl solution [32]. For this reason, aqueous solutions consisting of 0.05 M NH_4Cl (pH 4.5) with 1.5 mM Mn^{2+} were prepared and studied using cyclic voltammetry on MCFCNT electrodes to characterize the redox behavior of Mn. A flat background was seen for 0.05 M NH_4Cl in the range of 1400 mV to −1500 mV and hydrolysis started from −1500 mV. Then, the potential was cycled with 1.5 mM Mn^{2+} in 0.05 M NH_4Cl both from 0 mV to 1500 mV and from 1500 mV to −2000 mV to observe multiple relevant redox couples, as seen in Figure 1. As illustrated in the cyclic voltammogram, the reduction of Mn^{2+} starts at approximately −1000 mV with a peak width of 600 mV and a peak potential of −1300 mV, and the oxidation peak of deposited Mn is at −1250 mV. This peak location is compatible with ASV in the potential window of the MCFCNT electrode, so experiments were done to optimize the experimental conditions for ASV of Mn^{2+}.

3.1.2 pH and Deposition Potential Optimization—Osteryoung square wave mode was used for ASV measurements, and the first variable that was investigated was pH. Decreasing pH from 4.5 causes increasing peak current of Mn and for pH values lower than 3, evolution of hydrogen gas starts to significantly interfere with Mn electrodeposition on the electrode surface. The ASV analysis at pH 3 had the sharpest and highest peak current. Thus, pH 3 was selected for further optimization of ASV parameters for the measurement of Mn. The next parameter explored was deposition potential. This was done using 100 μM Mn in 0.05 M NH_4Cl (pH 3). As show in Figure 2, −1800 mV produces the sharpest peaks and largest peak current. At each potential, the measurements were done three times and the standard deviation is shown in Figure 2. The peak current drop for more negative deposition potentials is attributed to hydrogen gas evolution at the electrode surface which interferes with the mass transport of manganese analyte to the electrode surface. Thus, −1800 mV was selected as the most suitable deposition potential for further measurements.

3.1.3 Reproducibility and Cleaning Step Study—Between measurements, a constant potential of 600 mV was applied to thoroughly oxidize manganese residue on the electrode surface. After this step, the electrode showed reproducible behavior for CSV manganese detection.

3.1.4 Calibration Data—With a deposition time of 60 s, the peak height of stripping peaks shows a linear relationship in the concentration range from 3.5 μM to 13.5 μM with

the correlation equation I (μA)=(0.663±0.009) × [Mn (μmol)]−[(1.90±0.05) (μA)] and another linear range from 13.5 μM to 36.5 μM with the correlation equation I (μA)=(0.18±0.01)×[Mn (μmol)]+[(4.5±0.2) (μA)] as shown in Figure 3. Severe hydrogen evolution occurs in the manganese oxidation potential region, which leads to a distorted background for Mn voltammograms. The steep baseline causes the poorly-defined Mn stripping peaks since the manganese oxidation is superimposed on the hydrogen wave, which shifts positively as more Mn is deposited. The narrow linear range at lower concentration is due to saturation of the working electrode surface with a layer of Mn. The second linear range at higher concentration follows the mechanism of deposition of Mn on top of the base Mn layer which has a different slope as reflected in the calibration curve. Based on the first linear range, the limit of detection by ASV was calculated (3σ/slope) to be 120 nM. Also, under the same experimental conditions, a 10 min deposition was explored and longer deposition time does not change either the two linear range patterns or increase the sensitivity. Because of the relatively narrow linear range of detection and poorly defined peak shape within the detection range of ASV, CSV was investigated as an alternative technique for Mn detection.

3.2 CSV Study of Manganese

3.2.1 Cyclic Voltammetry of Mn in Borate Buffer—Cyclic voltammetry was first performed with Mn^{2+} to study the redox behavior of Mn^{2+} in a wide potential window. The accumulation of Mn is the oxidation of Mn^{2+} to MnO_2:

$$\mathrm{Mn^{2+}\,(H_2O)}_x(\mathrm{aq}) \leftrightarrow \mathrm{MnO_2\,(H_2O)}_{x-y}(\mathrm{s}) + 4\mathrm{H^+} + (y-2)\,\mathrm{H_2O} + 2\mathrm{e^-}$$

Since a basic medium helps the formation of MnO_2, borate buffer solution was selected as a basic buffer [15]. The voltammogram was first scanned from 0 to 1000 mV and then scanned from 1000 mV to −1000 mV and back to 0. Figure 4 shows two major reactions of Mn^{2+} on the CNT electrode in pH 8.5 borate buffer solution: oxidation of Mn^{2+} to MnO_2 at ca. 500 mV and reduction of Mn^{2+} to Mn at ca. −1400 mV. The reduction peak of Mn^{2+} is superimposed on the hydrolysis wave which, as discussed earlier, significantly interferes with ASV measurement of Mn^{2+}. On the other hand, the oxidation peak of Mn^{2+} is in a more central region of the potential window which has much less interference compared to the ASV method.

3.2.2 pH Optimization of Buffer Solution—Since the solubility of MnO_2 is quite dependent on solution pH, optimization of buffer pH is critical for reproducible and sensitive experimental results. Figure 5A shows how pH affects the CSV peak height of Mn^{2+}. It is observed that with a deposition potential of 600 mV at pH 8.5 in borate buffer, the CSV peak has a larger peak height and better looking peak shape than the ASV peak. Therefore, pH 8.5 was selected as the buffer pH for CSV measurements. Stripping peaks are observed to shift to a more negative potential as the pH becomes more basic. This is because the more acidic solution makes the reduction of MnO_2 easier by pushing the equilibrium to the right.

$$\mathrm{MnO_2\,(H_2O)}_{x,y}(\mathrm{s}) + 4\mathrm{H^+} + (y-2)\,\mathrm{H_2O} + 2\mathrm{e^-} \leftrightarrow \mathrm{Mn^{2+}\,(H_2O)}_x(\mathrm{aq})$$

3.2.3 Deposition Potential Optimization of CSV—A deposition potential study was performed in pH 8.5 borate buffer with 1 μM Mn^{2+} solution. Based on the CV of Mn^{2+} (Figure 4), 600 mV was chosen as the minimum deposition potential that would

preconcentrate MnO_2 onto the CNT electrode, and the deposition potential was investigated using increases of 50 mV up to 800 mV, as illustrated in Figure 5B. Increasing the potential did not change the size or shape of MnO_2 reduction, so 600 mV was chosen as the deposition potential for CSV.

3.2.4 Reproducibility and Cleaning Step Study—Similar to ASV measurements, a reproducibility test was carried out to establish a protocol for reliable CSV manganese measurements. Between measurements, a constant potential of −1500 mV was applied to the electrode for 2 min to thoroughly reduce manganese oxide. After this step, the electrode showed reproducible behavior for CSV manganese detection.

3.2.5 Calibration Data—CSV measurements of a series of Mn standards were performed under optimized conditions as described above in 0.1 M pH 8.5 borate buffer solution. Figure 6A shows the dynamic range of CSV measurements of Mn in the concentration range from 0.12 μM to 12 μM. Each measurement was done three times and the standard deviation is shown in Figure 6A. The linear range was from 0.6 to 6.7 μM and the correlation equation was I(μA)=(1.452±0.003)×[Mn (μmol)] − [(0.65±0.12) (μA)] (R^2=0.99 for 11 concentrations within the range). The limit of detection was calculated to be 93 nM (based on 3σ/slope). Figure 6B shows CSV stripping voltammograms of Mn with increasing Mn concentrations in the linear concentration range of 0.6–6.7 μM. Each voltammogram represents three replicas of measurements which behave similarly. A longer deposition time of 15 minutes under the same experimental condition gave a detectable concentration of 30 nM. 0.12 μM Mn solution was used to study how accumulation time affects Mn CSV behavior and the result is shown in Figure 7. It is seen that for an accumulation time less than 13 min, peak current follows a linear trend vs. accumulation time; as time increases, peak current starts to level off due to depletion of the analyte from the sample.

3.3 Natural Matrix of CSV Study of Manganese

In general, CSV has several advantages over ASV for Mn measurements on MCFCNT electrodes, such as lower limit of detection, better sensitivity and better reproducibility. To show that this method shows promise for Mn^{2+} detection in more complex matrices, a sample of natural water was run to evaluate this method in the presence of potential interferences. Burnet Woods (Cincinnati, OH) pond water was collected from shore using a plastic sampling bottle on November 11th 2011. There was no further treatment to the pond water and it was used immediately after collection as a natural water matrix into which Mn^{2+} was spiked. Atomic absorption spectroscopy showed no detectable Mn^{2+} in the unspiked sample. For CSV analysis the sample was adjusted to pH 8.5 using borate buffer. A 0.09 μM artificial Mn^{2+} sample was prepared by diluting AAS standard Mn solution (1000 ppm) into the buffered pH 8.5 pond water matrix and tested with the standard addition method using CSV (Figure 8). The peak current shows linear response vs. additions of Mn stock solution: I(μA)=(0.83±0.04)×[Mn (μmol)]+[(0.074±0.011) (μA)] (R^2=0.99). The result of Mn in the spiked sample was calculated to be 0.09±0.01 μM which is in close agreement with 0.09 μM.

4 Conclusions

We have evaluated two stripping voltammetry methods of detecting Mn^{2+} in aqueous solutions using metal catalyst free carbon nanotube electrodes. The ASV method we examined was shown to have a narrow linear range of detection and poor stripping peak shape. The CSV method that was explored as an alternative shows a lower limit of detection and better sensitivity. The CSV method was then shown to be a very reproducible and reliable technique for the detection of Mn^{2+}, and robust enough to operate in a sample such

as pond water. The MCFCNT electrode for CSV detection of Mn has a low limit of detection, wide linear range and good reproducibility. Previously, our lab has designed a bismuth film chip which was used for ASV detection of Mn in blood samples [33]. However, due to the high electronegativity of Mn, the limit of detection of Mn was only 5μM. Since MCFCNT has shown a promising CSV result for Mn detection, it can potentially be a coating material on this chip to provide a better limit of detection.

Acknowledgments

The authors gratefully acknowledge support provided by *NIEHS* R21ES019255 and *SCNTE LTD*.

References

1. Witholt R, Gwiazda RH, Smith DR. Neurotoxicol Teratol. 2000; 22:851. [PubMed: 11120391]
2. Hue NV, Vega S, Silva JA. Soil Sci Soc Am J. 2001; 65:153.
3. Colombini MP, Fuoco R. Talanta. 1983; 30:901. [PubMed: 18963494]
4. Kissinger, PT.; Heineman, WR., editors. Laboratory Techniques in Electroanalytical Chemistry. 2. Vol. ch 24. Marcel Dekker; New York: 1996.
5. Tölg G. Angew Chem Int Ed. 1986; 25:485.
6. Wang, J. Analytical Electrochemistry. 3. Vol. ch 3. Wiley; Hoboken, NJ, USA: 2006.
7. Tarley CRT, Santos VS, BaÞta BEL, Pereira AC, Kubota LT. J Hazard Mater. 2009; 169:256. [PubMed: 19398268]
8. O'Halloran RJ. J Anal Chim Acta. 1982; 140:51.
9. Barek J, Zima J. Electroanalysis. 2003; 15:467.
10. Achterberg EP, Braungardt C. Anal Chim Acta. 1999; 400:381.
11. Nolan MA, Kounaves SP. Anal Chem. 1999; 71:3567.
12. Wang J, Lu J, Hocevar SB, Farias PAM, Ogorevc B. Anal Chem. 2000; 72:3218. [PubMed: 10939390]
13. Wang J, Lu J. Talanta. 1995; 42:331. [PubMed: 18966234]
14. El-Maali NA, El-Hady DA. Anal Chim Acta. 1998; 370:239.
15. Hrabankova E, Dolezal J, Masin V. J Electroanal Chem. 1969; 22:195.
16. Labuda J, Vaníčková M, Beinrohr E. Microchim Acta. 1989; 1:113.
17. Roitz JS, Bruland KW. Anal Chim Acta. 1997; 344:175.
18. Saterlay AJ, Foord JS, Compton RG. Analyst. 1999; 124:1791. [PubMed: 10746310]
19. Di J, Zhang F. Talanta. 2003; 60:31. [PubMed: 18969022]
20. Baughman RH. Science. 2000; 290:1310. [PubMed: 17787234]
21. Hinds BJ, Chopra N, Rantell T, Andrews R, Gavalas V, Bachas LG. Science. 2004; 303:62. [PubMed: 14645855]
22. Dukovic G, Balaz M, Doak P, Berova ND, Zheng M, McLean RS, Brus LE. J Am Chem Soc. 2006; 128:9004. [PubMed: 16834352]
23. Huang S, Dai L, Mau AWH. J Phys Chem B. 1999; 103:4223.
24. Mathur RB, Seth S, Lal C, Rao R, Singh BP, Dhami TL, Rao AM. Carbon. 2007; 45:132.
25. Tibbetts GG, Meisner GP, Olk CH. Carbon. 2001; 39:2291.
26. Pumera M, Sasaki T, Iwai H. Chem Asian J. 2008; 3:2046. [PubMed: 18810741]
27. Niemann MU, Srinivasan SS, Phani AR, Kumar A, Goswami DY, Stefanakos EK. J Nanomater. 2008 ID 950967.
28. Jones CP, Jurkschat K, Crossley A, Compton RG, Riehl BL, Banks CE. Langmuir. 2007; 23:9501. [PubMed: 17655265]
29. Banks CE, Crossley A, Salter C, Wilkins SJ, Compton RG. Angew Chem Int Ed. 2006; 45:2533.
30. Yue W, Riehl BL, Pantelic N, Schlueter KT, Johnson JM, Wilson RA, Guo X, King EE, Heineman WR. Electroanalysis. 2012; 24:1039.

31. Osteryoung JG, Osteryoung RA. Anal Chem. 1985; 57:101A.
32. Lesven L, Skogvold SM, Mikkelsen Ø, Billon G. Electro-analysis. 2009; 21:274.
33. Jothimuthu P, Wilson RA, Herren J, Haynes EN, Heineman WR, Papautsky I. Biomed Microdevices. 2011; 13:695. [PubMed: 21479538]

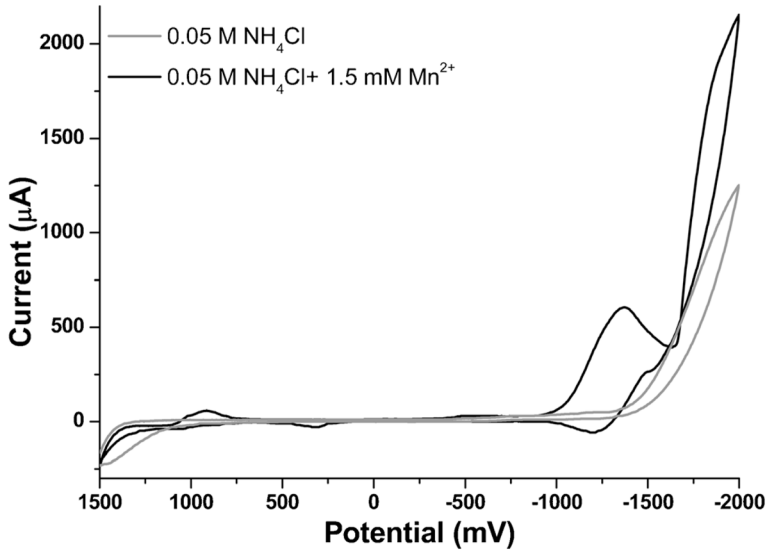

Fig. 1.

Cyclic voltammetry of 1.5 mM Mn^{2+} in 0.05 M NH_4Cl on MCFCNT electrode, scan rate 100 mV/s.

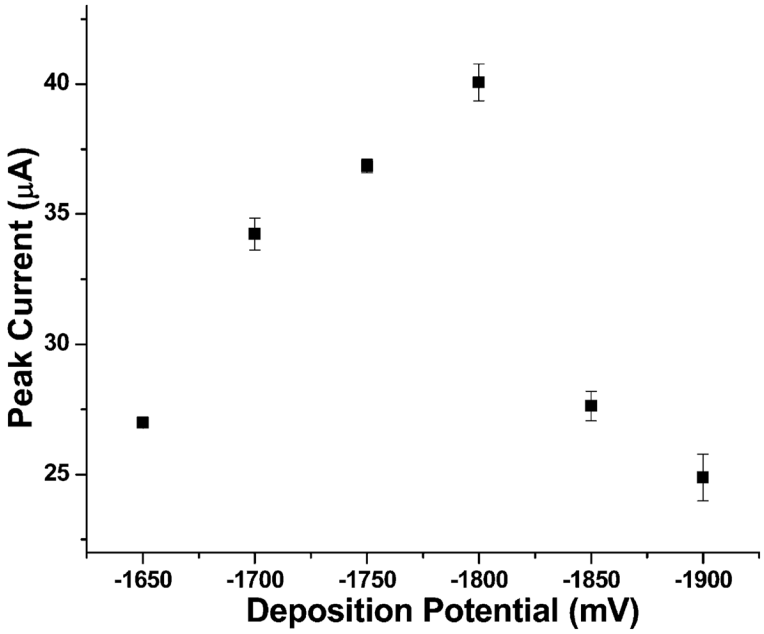

Fig. 2.
Deposition potential optimization of 100 μM Mn^{2+} in 0.05 M NH_4Cl.

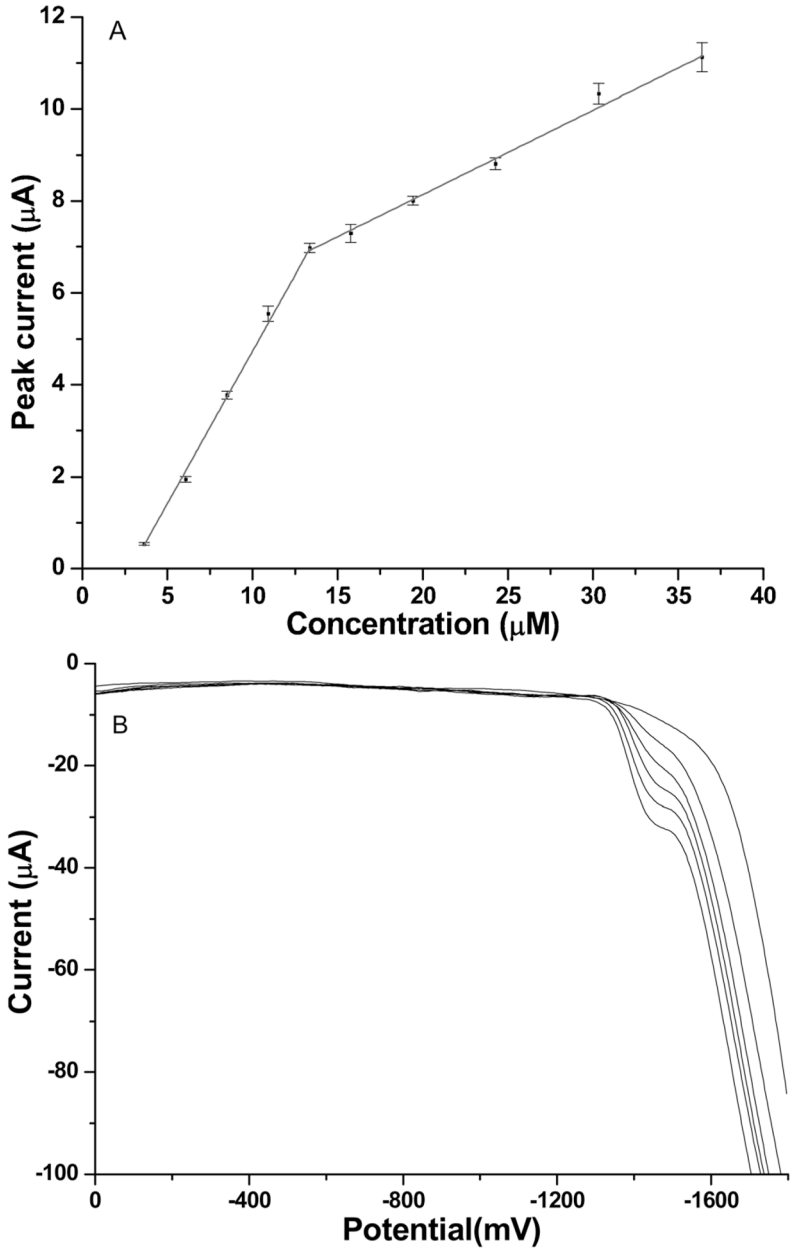

Fig. 3.

A) Calibration curve for anodic stripping voltammetry of Mn^{2+} in 0.05 M NH_4Cl; B) Anodic stripping voltammograms of Mn^{2+} in 0.05 M NH_4Cl in the concentration range of 3.5 μM to 13.5 μM.

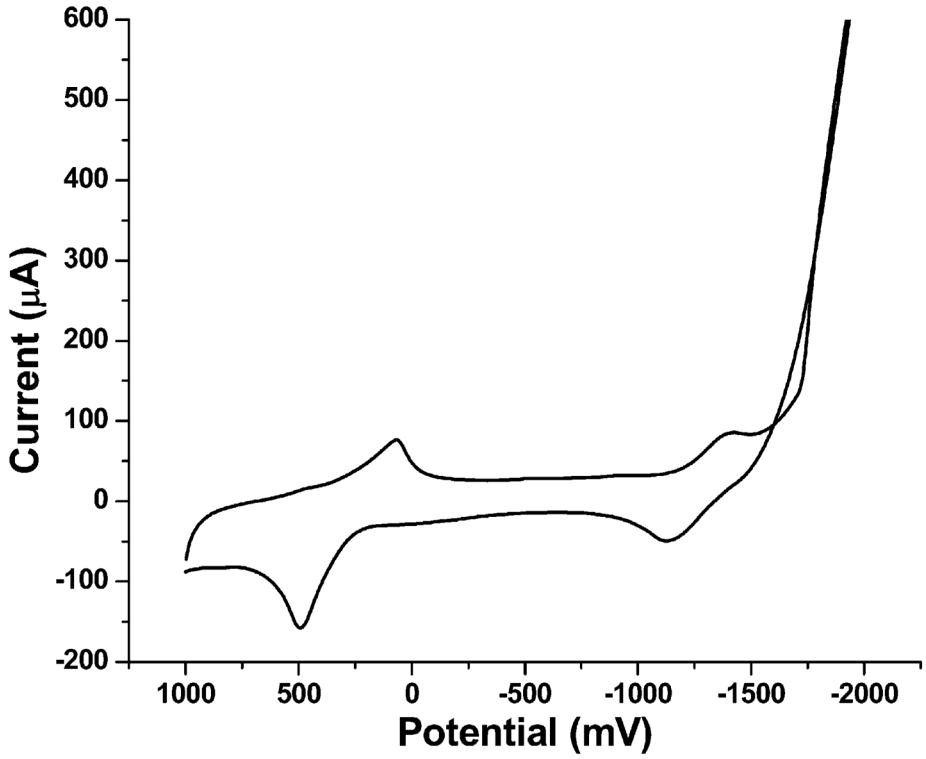

Fig. 4.
Cyclic voltammogram of 1.5 mM Mn^{2+} in 0.1 M pH 8.5 borate buffer, scan rate 100 mV/s.

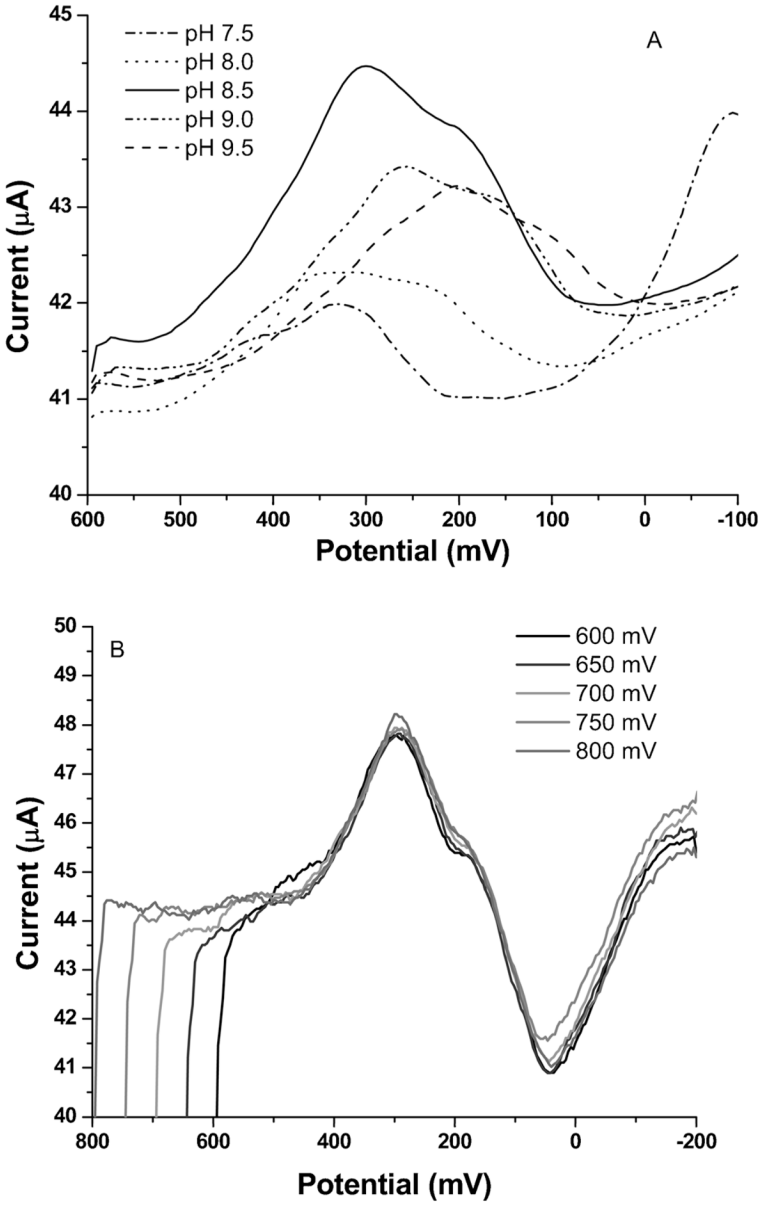

Fig. 5.

A) CSV pH optimization of Mn^{2+} from pH 7.5–9.5, deposition potential: 600 mV; B) CSV deposition potential optimization of Mn^{2+} from 600 mV to 800 mV, pH 8.5; Mn^{2+} concentration for A and B: 1 μM, deposition time for A and B: 60 s.

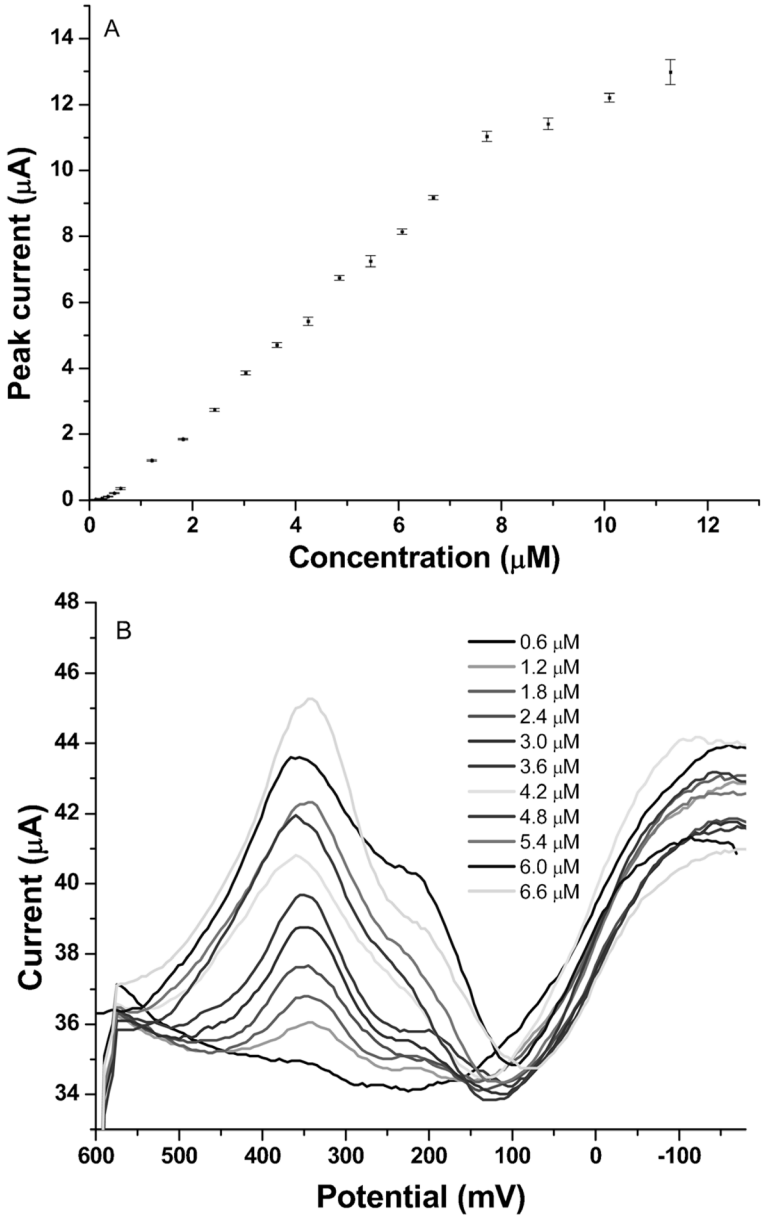

Fig. 6.

A) Calibration curve for CSV measurements of Mn in the range of 0.12 μM–12 μM; B) CSV stripping voltammograms of Mn in the range of 0.6–6.7 μM.

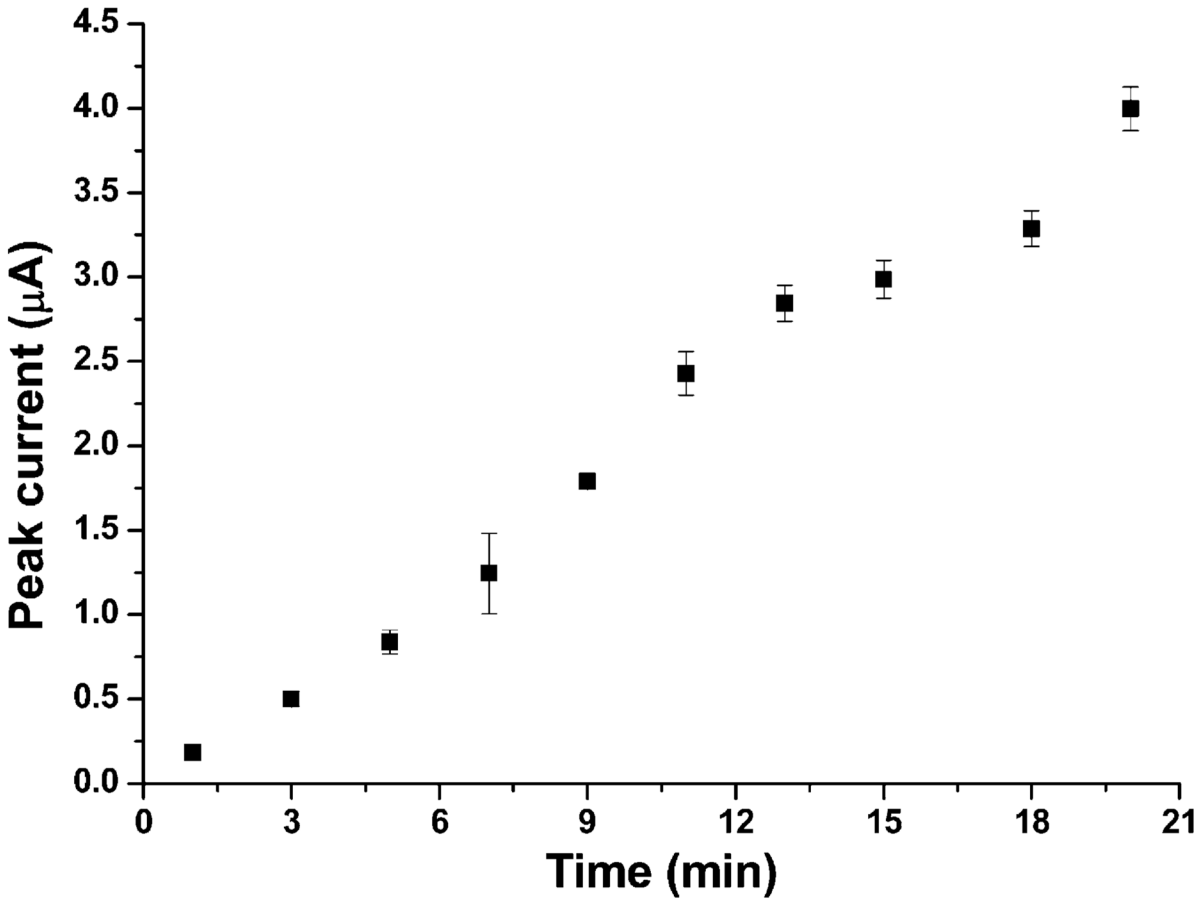

Fig. 7.

Accumulation time effect on peak current from 1–20 min; deposition potential: 600 mV; pH: 8.5; Mn concentration: 0.12 μM.

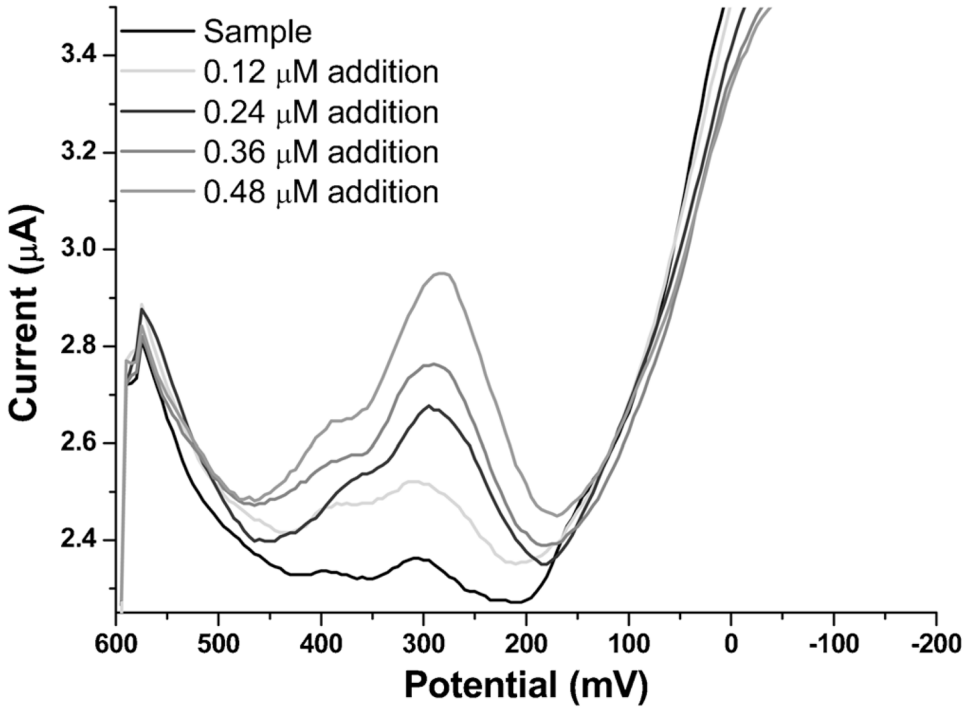

Fig. 8.

Voltammograms of CSV measurements of Mn in spiked pond water sample; deposition time: 60 s; deposition potential: 600 mV; pH: 8.5.